ATL-PHYS-PUB-2006-029

Sensitivity of ATLAS to FCNC single top quark production

T. L. Cheng† and P. Teixeira-Dias

Department of Physics, Royal Holloway, University of London, Egham, Surrey, TW20 0EX, UK

4 August 2006
(Revised: 29 July 2008)

Abstract

The anomalous production of single top quarks via flavour-changing neutral currents (FCNCs), $u(c) + g \to t$, is studied using the ATLAS detector at the Large Hadron Collider at CERN. Detector simulation is done using the fast simulation package ATLFAST. A number of important systematic effects have been addressed. Based on a cut-based analysis we show that with 10 fb^{-1} ATLAS can observe such top FCNC interactions with 5σ significance if the anomalous coupling strengths are $\kappa_g^u/\Lambda = \kappa_g^c/\Lambda \geqslant 0.0120^{+0.0014}_{-0.0012}$ (sys.) TeV^{-1}, or equivalently the branching ratios $\mathrm{BR}(t \to ug) + \mathrm{BR}(t \to cg) \geqslant 2.64^{+0.63}_{-0.51}$ (sys.)$\times 10^{-4}$. In terms of production cross section, such a discovery requires at least 13.7 pb of anomalous single top quark production. With this level of sensitivity, ATLAS will be able to test some models of new physics.

Keywords: top quark, FCNC, single top production, ATLAS, LHC.

† Now at H.H. Wills Physics Laboratory, University of Bristol, Tyndall Avenue, Bristol, BS8 1TL, UK. E-mail: t.l.cheng@bristol.ac.uk

1 Introduction

According to the standard model (SM), top quarks can only change flavour by means of charged current interactions with the W boson, but not via interactions with the neutral Z, γ, g gauge bosons at tree level. Such flavour-changing neutral currents (FCNCs) involving a top quark are induced by loop diagrams and are highly suppressed. These FCNC interactions are potentially very sensitive to new physics since new particles could be exchanged in the loop, leading to observable deviations from the SM.

The SM predicts the branching ratio of FCNC top decay $t \to qV$ ($q = u, c$; $V = Z, \gamma, g$) to be no larger than 10^{-12} (see Table 1). Such minuscule branching ratios mean that the decay is far too small to be observed in any collider experiments. Therefore any signal of top quark FCNC interactions would be strong evidence of new physics. There are many new physics models which allow top FCNC interactions at a much larger rate (several orders of magnitude), as can be seen in Table 1. Some of these predictions could be tested at the Large Hadron Collider (LHC) at CERN.

Table 1: Top quark FCNC decay branching ratios: SM predictions compared to potential values predicted by type III two-Higgs-doublet model (2HDM-III), Minimal Supersymmetric extension to the Standard Model (MSSM), R-parity violating MSSM ($\not{R}$-MSSM), and Topcolor-assisted Technicolor (TC2) models [1]. The numbers for SM and 2HDM-III are for decays into c quarks; the respective branching ratios for decays into u quarks are a factor $|V_{ub}/V_{cb}|^2 \sim 0.0079$ smaller.

	SM	2HDM-III	MSSM	$\not{R}$-MSSM	TC2
$t \to qg$	4.6×10^{-12}	10^{-4}	10^{-4}	10^{-3}	10^{-5}
$t \to q\gamma$	4.6×10^{-14}	10^{-7}	10^{-6}	10^{-5}	10^{-7}
$t \to qZ$	1×10^{-14}	10^{-6}	10^{-6}	10^{-4}	10^{-5}

At the LHC, the FCNC couplings $tq\gamma$ and tqZ are best studied in the decay mode. The tqg coupling, on the other hand, is best studied in the production mode since the decay $t \to qg$ is expected to be overwhelmed by the huge QCD dijets background. The subject of this note is to evaluate how sensitive is the ATLAS detector [2] to single top quark production via the FCNC coupling tqg with subsequent decay $t \to b\,\ell\nu$. We remark that throughout this note the word *lepton* and the symbol ℓ are used to refer to an electron (e) or a muon (μ). The full details of this study are reported in [3]. The Feynman diagram for the signal production and decay is shown in Figure 1. The first study of this channel with ATLAS can be found in Ref. [4], which was done using private codes implemented in the PYTHIA generator. The present work is performed using the publicly available generator

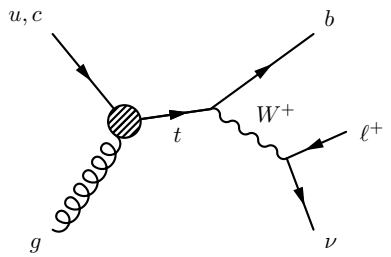

Figure 1: Signal production and decay: $u(c) + g \to t \to b\,W \to b\,\ell\nu$.

TOPREX [5], and is the first in-depth investigation of the sensitivity for the initial low-luminosity running of the LHC which includes a detailed discussion of the systematic uncertainties.

The top quark FCNC coupling to a gluon can be parameterized in a model-independent way using an effective Lagrangian, as follows [6]:

$$\mathcal{L} \;=\; -\,g_{\rm s}\sum_{q=u,c}\frac{\kappa_g^q}{\Lambda}\,\overline{t}\,\sigma^{\mu\nu}\,T^a\,(f_g^q+ih_g^q\gamma_5)\,q\,G^a_{\mu\nu}+{\rm h.c.}\;, \tag{1}$$

where $g_{\rm s}$ is the strong coupling, κ_g^q is a real and positive parameter representing the effective FCNC coupling[1], Λ is the new physics scale, $\overline{t}$ and q are quark spinor fields, T^a are the Gell-Mann matrices, $G^a_{\mu\nu}$ is $\partial_\mu G^a_\nu - \partial_\nu G^a_\mu$ (G^a_μ are the gluon fields), f and h are complex numbers satisfying $|f|^2+|h|^2=1$. (In this paper we use $f=h=1/\sqrt{2}$.)

From the effective Lagrangian in Eq. (1), the top quark decay width for $t\to qg$ ($q=u,c$) can be calculated as a function of the top quark FCNC couplings [6]:

$$\Gamma(t\to qg)=\left(\frac{\kappa_g^q}{\Lambda}\right)^2\,\frac{8}{3}\,\alpha_{\rm s}\,m_t^3. \tag{2}$$

The equation above will be used later to calculate the anomalous FCNC branching ratio for a given coupling κ. The current upper limits on the anomalous couplings are established by the D0 Collaboration at the Tevatron: $\kappa_g^u/\Lambda < 0.037$ TeV^{-1} (at 95% confidence level), $\kappa_g^c/\Lambda < 0.15$ TeV^{-1} [7]. These should correspond to limits on the branching ratios of ${\rm BR}(t\to ug) < 1.3\times10^{-3}$ and ${\rm BR}(t\to cg) < 2.0\times10^{-2}$ [5]. Note that the definition of the coupling κ is not unique, hence comparisons are best made using branching ratios.

In this study we assume $m_t = 175$ GeV/c^2 and $m_W = 80.425$ GeV/c^2. We set the default value of κ_g^q and Λ to be $\kappa_0 = 0.01$ and $\Lambda_0 = 1$ TeV respectively. With $\alpha_{\rm s}(m_t) = 0.1$, we find that $\Gamma(t\to ug)=\Gamma(t\to cg)=0.1429$ MeV/$\hbar$, and the corresponding FCNC branching ratio is ${\rm BR}(t\to ug)={\rm BR}(t\to cg)=9.04\times10^{-5}$ (assuming equal tug and tcg couplings). With the default coupling the predicted cross section for FCNC single top quark production is 8.0 pb (1.6 pb) for $ug\to t$ ($cg\to t$) [5].

2 Signal and background

2.1 Discussion of signal and background processes

We only consider the semileptonic decay, $t\to bW\to b\,\ell\nu$, since the lepton can be used as a trigger. Hence the experimental signature for the signal is the presence of an isolated lepton, a b-tagged jet (from now on referred to as b-jet) originating from the b-quark, and large missing transverse momentum. In addition, there will be QCD jets not related to the hard scattering. The search strategy is to reconstruct the top quark mass and look for an excess of events at the mass peak.

In this paper, we consider two signal subprocesses depending on the flavour of the incoming quark. The production of top quarks and anti-quarks from up type quarks, $u(\overline{u})g\to t(\overline{t})$, will be referred to simply as 'ug', while that from charm quarks, $c(\overline{c})g\to t(\overline{t})$ as 'cg'.

[1] In this paper we use the notation κ_g^q corresponding to the tqg effective coupling, as adopted elsewhere (e.g. Reference [7]). The alternative and equivalent notation κ_{tq}^g is not used here.

The signal is expected to suffer from three categories of background: top-background, in which top quarks are produced via SM couplings; W-background, where a real W boson is produced; and background from QCD heavy quark pair production. The individual background processes studied are discussed below:

Electroweak single top production This is irreducible because it has characteristics very similar to the signal. In the lowest order in SM, there are three ways to produce a top quark: (i) with a virtual t-channel W ('t-channel'), (ii) in association with a real W boson ('tW'), and (iii) with a virtual s-channel W ('s-channel'). The t-channel has the largest cross section ($\sim$ 250 pb [8]) and is an important background. The latter two are negligible.

Top quark pair production ($t\bar{t}$) This is a background when one top decays semileptonically while the other decays hadronically. Although the cross section ($\sim$ 800 pb [6]) is significantly larger than the single top production, a large rejection factor (10^4) can be achieved since the two top quarks are typically much more boosted than in the signal.

Production of W plus b-quark pair ($Wb\bar{b}$) This is a background when one b-quark jet is tagged while the other is not (possibly escaping into the forward region, $|\eta| > 2.5$). The expected cross section is $\sigma \times \mathrm{BR}(W \to \ell\nu) \sim 70$ pb [5].

Production of W plus c-quark pair ($Wc\bar{c}$) When one of the c-jets is mistaken as a b-jet, $Wc\bar{c}$ events would mimic the signal. This process has a cross section of $\sigma \times \mathrm{BR}(W \to \ell\nu) \sim 260$ pb [5].

Production of W plus light-jets (W+jets) At the LHC, a huge number of W bosons will be produced along with a number of light-quark and gluon jets (hereafter referred to as *light-jets*). The exclusive cross section including the $W \to \ell\nu$ decay is ~ 9 nb in the phase space of interest.[2] W+jets events become a background when a jet is mis-identified as a b-jet.

QCD heavy quark production Background could also arise from heavy quark production such as $b\bar{b}$ and $c\bar{c}$, where one heavy quark undergoes semileptonic decay and produces a lepton and a neutrino. Since these leptons are either slow or not isolated, a huge rejection factor of heavy quark events can be obained. Note that although the inclusive production cross sections of $c\bar{c}$ is larger than $b\bar{b}$, both cross sections are of similar size (few microbarns) in the relevant phase space [3].

Background could also arise from QCD processes such as dijet production in which a jet is faking an electron. These backgrounds are not simulated in this study because fake electrons are not treated in the fast simulation.

However, thanks to the excellent electron/jet separation in ATLAS (fake electron rate is $\sim 10^{-5}$) [9], which is enough to eliminate most QCD processes, the contribution from fake electrons is expected to be small compared to the top- and W-backgrounds.

[2] Obtained from PYTHIA for W bosons with a minimum transverse momentum of 20 GeV/c in the hard interaction.

Table 2: Event generation information for signal and background processes. All cross sections are obtained from generators and are inclusive, except W+jets, $b\bar{b}$, and $c\bar{c}$ where a generator cut on the minimum transverse momentum of the particles produced in hard interatction is applied (20, 20, 25 GeV/c respectively). Cross sections for the W-backgrounds include BR($W \to \ell\nu$). Cross section values are leading order except those in parentheses which are from NLO/NLL analytical calculations. The last column lists the total number of MC events generated.

Label	Physics process	Cross section	Size
ug	$ug \to t \to bW$	8.0 pb	2M
cg	$cg \to t \to bW$	1.6 pb	0.8M
t-ch.	$qb \to q't \ + \ qg \to q't\bar{b}$	270 (246.6) pb	2M
tW	$gb \to tW$	52 pb	1.2M
s-ch.	$q\bar{q}' \to W^* \to t\bar{b}$	7.0 (10.65) pb	0.8M
$t\bar{t}$	$gg + q\bar{q} \to t\bar{t}$	490 (886) pb	10M
$Wb\bar{b}$	$q\bar{q}' \to Wb\bar{b}$	71.14 pb	1.2M
$Wc\bar{c}$	$q\bar{q}' \to Wc\bar{c}$	263.2 pb	5.2M
W+jets	$q\bar{q}' \to Wg \ + \ qg \to W\bar{q}'$	8.971 nb	20M
$b\bar{b}$	$gg + q\bar{q}' \to b\bar{b}$	3.4 μb	300M
$c\bar{c}$	$gg + q\bar{q}' \to c\bar{c}$	1.4 μb	240M

2.2 Simulation of data samples

Simulation of proton-proton collisions at the LHC is performed assuming $\sqrt{s} = 14$ TeV and low luminosity ($10^{33}\text{cm}^{-2}\text{s}^{-1}$). Most of the physics processes were simulated using the TOPREX 4.10 [5] Monte Carlo (MC) event generator for the hard scattering, and PYTHIA 6.226 [10] for the simulation of parton shower, hadronization and decay of unstable particles. The exceptions are W+jets, $b\bar{b}$, and $c\bar{c}$ which were generated using PYTHIA alone. Both TOPREX and PYTHIA use leading order (LO) matrix elements. Some of the event generation information is given in Table 2, the cross section values obtained from the generators and the size of the MC data sample. Note that next-to-leading order (NLO) cross sections from Ref. [8] are used to normalize the t- and s-channel single top production cross section, while the next-to-leading logarithmic resummed (NLO+NLL) cross section from [6] is used for $t\bar{t}$ production.

The renormalization scale (μ_R) and factorization scale (μ_F) are set to equal values μ_0: for the signal and background single top processes we used $\mu_0 = m_t$; for $t\bar{t}$ $\mu_0 = \sqrt{p_\perp^2 + m_t^2}$; for $Wb\bar{b}$ and $Wc\bar{c}$ $\mu_0 = m_W$; for W+jets, $b\bar{b}$ and $c\bar{c}$, the PYTHIA default is used: $\mu_0 = \sqrt{p_\perp^2 + (m_3^2 + m_4^2)/2}$ (m_3 and m_4 are the masses of the two particles emerging from the hard scattering).

In the event generation of the signal process, only $t \to bW$ is simulated (allowing all subsequent W decays). In comparison, all decay modes of top (and W) are simulated for the top-backgrounds while for the W-backgrounds, we only simulated $W \to \ell\nu$ to improve efficiency. Contribution from $W(\to \tau\nu)$+jets has been verified to be small and has only a small effect on the result [3].

For the nominal data sample, the CTEQ5L [11] parton distribution function (PDF) is used. Simulation of the initial and final state QED and QCD radiation (ISR and FSR) is

included. Finally, the ATLAS tuning for the simulation of minimum bias and underlying event in PYTHIA is used [12].

The fast simulation program ATLFAST [13] is used to simulate the response of the ATLAS detector. The program employs parameterized resolution functions to simulate isolated leptons, photons, reconstruct jets, and estimate missing transverse energy. Tagging of heavy flavours (b-jet, c-jet, and τ) and jet energy calibration are also simulated. We use the standard b-tagging setting which yields a b-tagging efficiency of 60%, charm-jet mistagging probability of 10%, and light-jet mistagging probability of 1%.

3 Signal event selection

The initial event selection cuts applied to obtain an initial sample are listed below:

- Require one and only one isolated[3] lepton with $p_{\mathrm{T}} > 20$ GeV/c, $|\eta| < 2.5$,
- Require one and only one b-jet with $p_{\mathrm{T}} > 30$ GeV/c, $|\eta| < 2.5$,
- Require missing transverse momentum ($\not{p}_{\mathrm{T}}$) > 20 GeV/c,
- Veto extra isolated lepton ($p_{\mathrm{T}} > 5$ GeV/c (e), 6 GeV/c (μ); $|\eta| < 2.5$),
- Veto extra b-jet ($p_{\mathrm{T}} > 15$ GeV/c, $|\eta| < 2.5$).

Some distributions after these initial cuts are shown in Figures 2 and 3. Figure 2 shows the $\ell\nu$ transverse mass for the signal and a representative QCD background ($b\overline{b}$). It is clear that QCD backgrounds can be rejected very efficiently by imposing a lower bound in $m_{\mathrm{T}}(\ell, \nu)$. Figure 3 compares four distributions of the signal and total background (except QCD): (a) jet multiplicity (including b-jet), (b) transverse momentum of the b-jet, (c) invariant mass of the b-jet–lepton system, $m_{b\ell}$, and (d) scalar sum of the transverse momentum of all objects, $H_{\mathrm{T}} = p_{\mathrm{T}\ell} + \not{p}_{\mathrm{T}} + \sum^{\mathrm{alljet}} p_{\mathrm{T}}$.

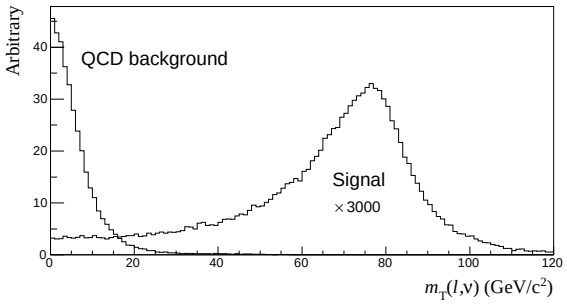

Figure 2: The $\ell\nu$ transverse mass distribution for signal and $b\overline{b}$ events after initial cuts.

After the initial cut, top quark candidates are reconstructed by constraining the invariant mass of the lepton-neutrino system to the known PDG mass of the W boson [14], i.e. $m_{\ell\nu} = m_W = 80.425$ GeV/c^2. The neutrino transverse momentum $p_{\nu\mathrm{T}}$ is assumed to be the total missing transverse momentum of the event. The solution for the longitudinal momentum of the neutrino, $p_{\nu\mathrm{L}}$, is given by:

[3] The isolation conditions are: (i) the lepton is separated from other calorimeter clusters ($E_{\mathrm{T}} > 10$ GeV) by at least $\Delta R = 0.4$ ($\Delta R = \sqrt{(\Delta\phi)^2 + (\Delta\eta)^2}$), and (ii) there is not more than 10 GeV transverse energy deposited within a cone of $\Delta R = 0.2$ around the lepton.

$$p_{\nu\mathrm{L}}^{(\pm)} \;=\; \frac{\lambda}{{p_{\nu\mathrm{T}}}^2}\left(p_{\ell\mathrm{L}} \pm \sqrt{|\mathbf{p}_\ell|^2\left(1-(\frac{p_{\nu\mathrm{T}}\,p_{\ell\mathrm{T}}}{\lambda})^2\right)}\right), \tag{3}$$

in which $\lambda \equiv \frac{1}{2}(m_W^2 - m_\ell^2) + \mathbf{p}_{\ell\mathrm{T}} \cdot \mathbf{p}_{\nu\mathrm{T}}$, and the $\mathbf{p}$'s are the momentum vectors.

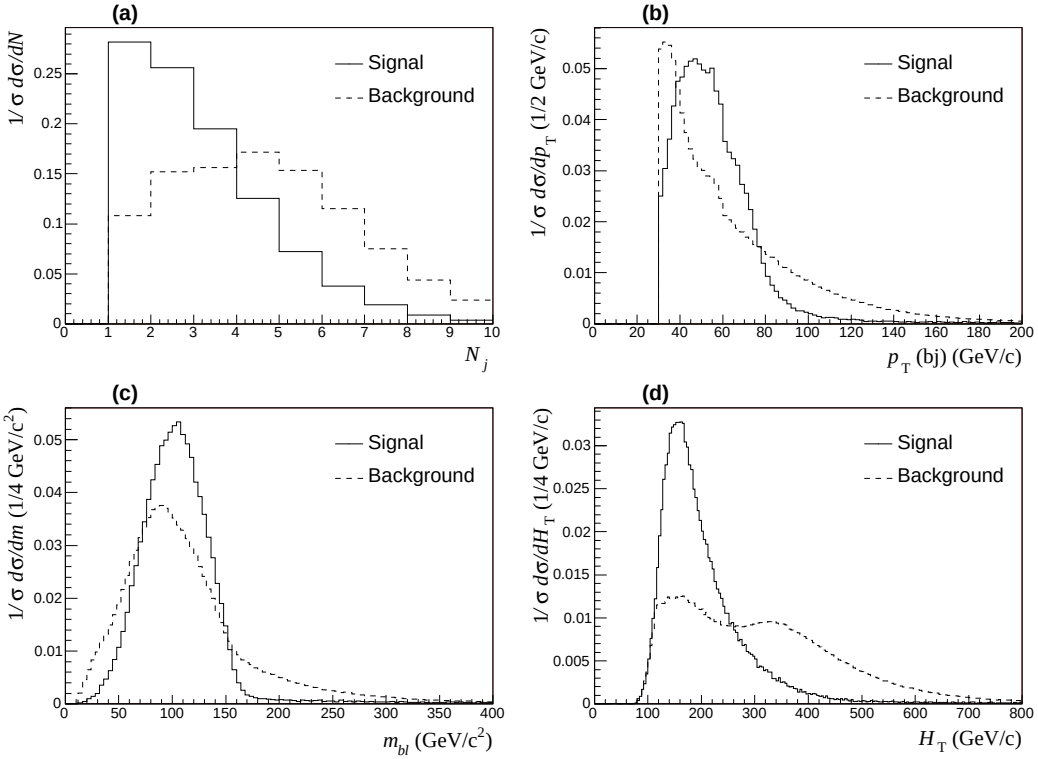

Figure 3: Comparing distributions of signal and total background (excluding QCD backgrounds) after the initial cuts: (a) N_j, (b) p_T(bj), (c) $m_{b\ell}$, and (d) H_T. Histograms are normalized to unit area. See text for definitions.

A consistent approach has been adopted to select one solution, i.e. by taking the solution with the smallest modulus, $|p_{\nu\mathrm{L}}|$. In the less likely case where no real solution was found—$p_{\nu\mathrm{L}}$is imaginary—then the real part of the solution was taken. On average this approach gives the correct solution 68% of the time for the ug signal.

Since the signal is an s-channel process simulated using a 2→1 matrix element, the produced top quark has little transverse momentum. To avoid being sensitive to NLO corrections, we only accept events which have a reconstructed top quark with p_T up to 20 GeV/c. It is interesting to note that in the standard model, such s-channel production of top quarks does not exist. Therefore the p_T of the top quarks is potentially a very important handle to disentangle the FCNC single top production from the SM counterparts.

Several observables were studied in order to find distributions which have the most discriminating power against the background. After these observables were found, the cuts were optimized in order to yield the highest signal significance, which is defined to be $S \equiv s/\sqrt{b}$, where s and b are the expected number of signal and background events for an integrated luminosity of 10 fb^{-1}. The optimization is carried out using the first half of the data sample; the second half is used to derive the sensitivity limits.

The set of optimized cuts used to obtain the final result is listed below:

- Transverse mass of the reconstructed W, $m_{\mathrm{T}}(\ell, \nu) > 25$ GeV/c^2,
- Require the b-jet to be the leading jet (i.e. the highest p_{T} jet),
- Transverse momentum of reconstructed top quark, $p_{\mathrm{T}}(t) < 20$ GeV/c,
- Transverse momentum of b-jet, $p_{\mathrm{T}}(bj) > 40$ GeV/c,
- Invariant mass of b-jet–lepton system, $m_{b\ell} > 55$ GeV/c^2,
- Scalar sum of transverse momentum, $H_{\mathrm{T}} < 270$ GeV/c,
- Transverse momentum of reconstructed W boson, $p_{\mathrm{T}}(W) > 34$ GeV/c,
- Reconstructed top quark mass, 135 GeV/c^2 $< m_t^{\mathrm{rec}} <$ 200 GeV/c^2.

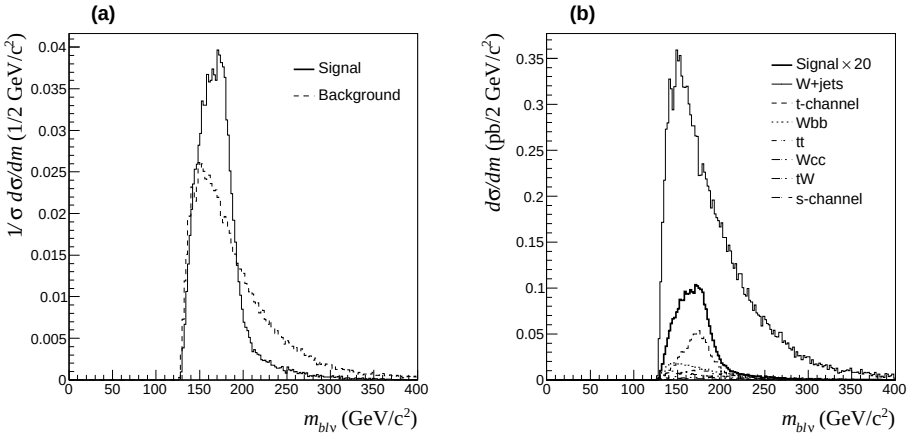

Figure 4: Reconstructed top quark mass distributions after all but the m_t^{rec} cut: (a) Signal vs. total background (excluding QCD backgrounds) (normalized), (b) Signal vs. each background (note signal is multiplied by a factor of 20).

The reconstructed top mass distribution is shown in Figure 4. Note that the peak position has shifted downward by ~ 10 GeV/c^2. This is mainly caused by the bias introduced by the method of selecting the solution for the neutrino longitudinal momentum, and partly caused by the under-estimation of b-jet energy due to out-of-cone activity.

The acceptance efficiencies (with respect to the number generated) after each of these cuts are given in Table 3. The final selection efficiency for signal is 1.08% for ug and 1.81% for cg.

The higher efficiency for cg can be understood by considering the different kinematics of the valence up quarks and that of $\overline{u}$, c, and $\overline{c}$ sea quarks. Since valence quarks have higher Bjorken-x than sea quarks, top quarks produced by the up quarks are more boosted than those produced by the sea quarks. Therefore the decay products, namely lepton and b-jet, are more likely to fall outside the pseudorapidity acceptance in the case of ug subprocess (see Figure 5). The implication is that efficiency for $ug \to t$ is less than the other three subprocesses, and the latter three should have approximately the same acceptance efficiencies. This is indeed the case: acceptance efficiencies after the initial cuts are 3.2%, 5.7%, 6.0%, and 6.0% for the case of ug, $\overline{u}g$, cg, and $\overline{c}g$ respectively. Hence after adding the charge conjugate subprocesses, efficiency for $c(\overline{c})g$ is considerably higher than $u(\overline{u})g$.

Table 3: Cumulative and inclusive acceptance efficiency after each cut (Note: † BR($t \to bW$) included; ‡ BR($W \to \ell\nu$) included.)

Cut	Initial	$m_{\rm T}(W)$	leading b	$p_{\rm T}(t)$	$p_{\rm T}(bj)$	$m_{b\ell}$	$H_{\rm T}$	$p_{\rm T}(W)$	$m_t^{\rm rec}$
$ug^\dagger$	3.65%	3.38%	2.90%	1.70%	1.42%	1.36%	1.28%	1.22%	1.08%
$cg^\dagger$	6.02%	5.59%	4.82%	2.83%	2.31%	2.22%	2.16%	2.05%	1.81%
t-chan.	5.90%	5.40%	3.07%	0.61%	0.54%	0.49%	0.47%	0.45%	0.39%
tW	10.14%	8.86%	4.38%	0.54%	0.49%	0.47%	0.27%	0.26%	0.13%
s-chan.	5.41%	4.86%	3.04%	0.53%	0.48%	0.44%	0.36%	0.35%	0.27%
$t\bar{t}$	10.01%	8.74%	3.49%	0.21%	0.20%	0.19%	0.05%	0.05%	0.03%
$Wb\bar{b}^\ddagger$	1.18%	1.13%	0.98%	0.57%	0.29%	0.26%	0.23%	0.21%	0.14%
$Wc\bar{c}^\ddagger$	0.15%	0.15%	0.13%	0.07%	0.03%	0.03%	0.03%	0.02%	0.02%
W+jets‡	0.20%	0.19%	0.15%	0.08%	0.04%	0.04%	0.04%	0.03%	0.02%
$b\bar{b}$	1.2×10^{-4}	2.4×10^{-6}	1.9×10^{-6}	4.6×10^{-7}	2.0×10^{-7}	2.0×10^{-7}	2.0×10^{-7}	1.7×10^{-7}	1.3×10^{-7}
$c\bar{c}$	2.3×10^{-6}	7×10^{-7}	3×10^{-8}	2×10^{-8}	2×10^{-8}	2×10^{-8}	2×10^{-8}	8×10^{-9}	0

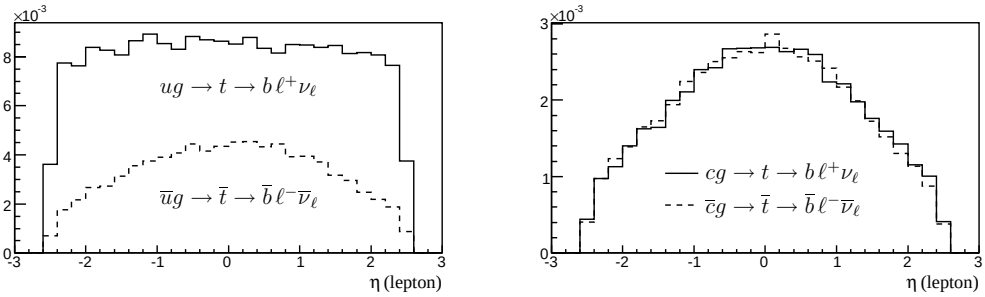

Figure 5: Lepton pseudorapidity distribution for ug (left) and cg (right) signal channels after the initial cuts.

After applying all selection cuts, the total (inclusive) signal efficiency (ε_s) is 1.20% while the total background rejection is 10^6 (ε_b=2.4×10^{-6}). The approximate expected number of signal and background events for 10 fb^{-1} are: 862 ug and 292 cg; 86 000 W+jets, 9 700 t-channel, 4 500 $Wb\bar{b}$, 4 000 $b\bar{b}$, 2 400 $t\bar{t}$, 1 900 $Wc\bar{c}$, 690 tW, and 290 s-channel. (The QCD dijets background should not exceed 1 000 events given the hypothesis on the jet fake rate of 10^{-5} and the mistag rate of 1%.) It is clear that W+jets is by far the dominant background, followed by t-channel single top production.

Thus the optimized signal significance for the nominal signal sample is $S_0 = 3.49 \pm 0.03$ ($1\,154 \pm 9$ signal events ($ug + cg$) and $109\,158 \pm 1\,272$ background events are expected for 10 fb^{-1}; the errors are due to the finite size of the simulated data samples).

4 Sensitivity limits

In this paper, two significance levels are considered: 5σ required for discovery, and 1.645σ for setting a one-sided 95% confidence level (CL) limit when no signal is found. The number of background events for 10 fb^{-1} is expected to fluctuate statistically by an amount $\sqrt{b}$, i.e. 330 events. Therefore, to reach a significance of 5σ we need to observe at least

1 652 signal events; if no more than 543 signal events are seen, then a 95% CL limit could be set.

These limits will be calculated for three different scenarios:

(1) Assuming *both tug* and *tcg* couplings are present and equal, $\kappa_g^q \equiv \kappa_g^u = \kappa_g^c \neq 0$,

(2) Assuming *only* the *tug* coupling is present, $\kappa_g^u \neq 0$, $\kappa_g^c = 0$,

(3) Assuming *only* the *tcg* coupling is present, $\kappa_g^u = 0$, $\kappa_g^c \neq 0$.

The signal production cross section required for each significance level can be computed for the three scenarios using $\sigma_s = s/(\varepsilon_s \int \mathcal{L}\, dt)$, where ε_s is the inclusive signal efficiency. To obtain a 5σ evidence in 10 fb^{-1} of data, the inclusive signal cross section needs to be at least 13.7 pb. If no evidence of signal is found then ATLAS could establish an exclusion limit of $\sigma_s < 4.5$ pb at 95% CL. The complete results for all scenarios are given below:

	ε_s (%)	5σ	95% CL
Scenario 1	1.20 ± 0.01	$\geqslant 13.7$ pb	< 4.5 pb
Scenario 2	1.08 ± 0.01	$\geqslant 15.3$ pb	< 5.0 pb
Scenario 3	1.82 ± 0.01	$\geqslant 9.1$ pb	< 3.0 pb

To derive the sensitivity on the underlying anomalous coupling, we observe that the significance is proportional to the effective signal cross section which includes the bW decay branching ratio. Since the inclusive cross section scales as $\sigma(qg \to t) \propto (\kappa/\Lambda)^2$, we have

$$\begin{aligned} S &\propto \sigma(qg \to t) \times \mathrm{BR}(t \to bW) \\ &\propto (\kappa/\Lambda)^2 \times \mathrm{BR}(t \to bW; \kappa/\Lambda). \end{aligned} \tag{4}$$

From this it is trivial to derive the following relation to compute the corresponding coupling κ/Λ needed for any given significance S:

$$\frac{\kappa}{\Lambda} = \frac{\kappa_0}{\Lambda_0} \sqrt{\frac{S}{S_0} \cdot \frac{\mathrm{BR}(t \to bW; \kappa_0/\Lambda_0)}{\mathrm{BR}(t \to bW; \kappa/\Lambda)}}. \tag{5}$$

From the derived limit on the coupling, the corresponding anomalous branching ratio can be computed using Eq. (2) as follows:

$$\Gamma(t \to qg) = 1.429\ (\kappa_g^q/\Lambda)^2\ (\mathrm{GeV}/\hbar), \tag{6}$$

$$\mathrm{BR}(t \to qg) = \frac{\Gamma(t \to qg)}{\Gamma_{\mathrm{SM}} + \Gamma(t \to qg)}, \tag{7}$$

where Γ_{SM} is the total top decay width in the standard model, $\Gamma_{\mathrm{SM}} = \Gamma(t \to bW, sW, dW) = 1.552$ GeV/$\hbar$.

It follows that in Scenario 1, where both *tug* and *tcg* couplings are equal, we would need $\kappa_g^q/\Lambda \geqslant 0.0120$ TeV^{-1}, or $\mathrm{BR}(t \to ug) + \mathrm{BR}(t \to cg) \geqslant 2.64{\times}10^{-4}$ for 5σ; in the absence of signal, the limits $\kappa_g^q/\Lambda < 0.0069$ TeV^{-1}, or $\mathrm{BR}(t \to ug) + \mathrm{BR}(t \to cg) < 8.67{\times}10^{-5}$, can be set at 95% CL. The complete results including those for Scenarios 2 and 3 will be given later in Table 7. The MC statistical uncertainty on the coupling limit is estimated to be of order 1%, and twice as large for the branching ratio.

5 Systematic uncertainties

The sensitivity limit is subject to various systematic uncertainties. These arise from the inaccuracy in the modelling of the physics processes as well as the detector, and also from reconstruction procedures of the physics events. (QCD backgrounds will not normally be included in the evaluation of systematic uncertainties because the required CPU time to produce new samples is unfeasibly long; but this should have little impact on the result since the QCD backgrounds make up only about 4% of the background.)

5.1 Theoretical uncertainty

Predictions made by a given theoretical model, e.g. the standard model, are not unique because of their dependency on a number of input parameters. These theoretical inputs may affect the overall cross section of a physics process as well as the shape of the distributions of variables used in the event selection. In this study, we consider the following inputs: (i) $\mu_{\rm R}$, (ii) $\mu_{\rm F}$, (iii) PDF, and (iv) m_t (for top-quark processes). By changing each of these inputs in the MC generator, we present an estimate for the theoretical systematic uncertainty on cross sections for all processes except for processes where NLO cross sections are used. (The effect on the distributions of variables used in event selection is not addressed.) The four inputs are briefly discussed below:

(i) $\mu_{\rm R}$ — This is the energy scale at which the strong coupling constant is evaluated. To estimate the systematic uncertainty, the scale is varied within the conventional range $\mu_0/2$–$2\mu_0$ [15] around the central value μ_0 (with $\mu_{\rm F}$ fixed). The uncertainty is then taken asymmetrically to be the maximum deviation in the cross section. The result is shown in Figure 6 (closed circles). The uncertainty is typically of $\mathcal{O}(10\%)$.

(ii) $\mu_{\rm F}$ — This is the energy scale at which parton distribution functions are evaluated. Similarly, the scale is varied within $\mu_0/2$–$2\mu_0$ (with $\mu_{\rm R}$ fixed) and the maximum deviation is taken to be the systematic uncertainty (see Figure 6 (open circles)). The uncertainty ranges from 2% to 12%.

(iii) PDF — To estimate the systematic uncertainty on the cross section due to parameterization of the parton distribution, three other PDFs, namely CTEQ5M1 [11], MRST2001-LO [16], and MRST2002-NLO [17] were used. The systematic uncertainty is taken conservatively to be the maximum cross section deviation and is treated as symmetrical. It ranges from 5% to 26%.

(iv) Input top quark mass — For processes involving top quarks, the input top mass can affect the cross section values. An uncertainty of $\delta m_t = \pm 2$ GeV/c^2 is assumed and the resulting uncertainties in cross section are estimated to be $\lesssim 3\%$.[4]

A summary of the aforementioned systematic uncertainties is given in Table 4. The total uncertainty is also given and is obtained by adding the four contributions in quadrature.

For t- and s-channel single top production, the theoretical uncertainty is taken from Ref. [8], i.e. $^{3.76}_{4.12}\%$ and $^{+6.08}_{-6.03}\%$ respectively. For $t\bar{t}$ and $b\bar{b}$ production, the uncertainty is conservatively taken to be ± 109 pb [6] and $^{+100}_{-50}\%$ [19] respectively.

After error propagation, the systematic uncertainty on the derived coupling κ induced by $\Delta\sigma$ is estimated, i.e. $^{+8.3}_{-7.8}\%$ from signal and $^{+3.4}_{-3.1}\%$ from background.

[4] A precision of 0.8% (1.4 GeV/c^2) has been achieved with the Run-II data at Tevatron [18]. At LHC, 2 GeV/c^2 precision is achievable with one year low luminosity and ultimately 1 GeV/c^2 is possible with high luminosity beam [2].

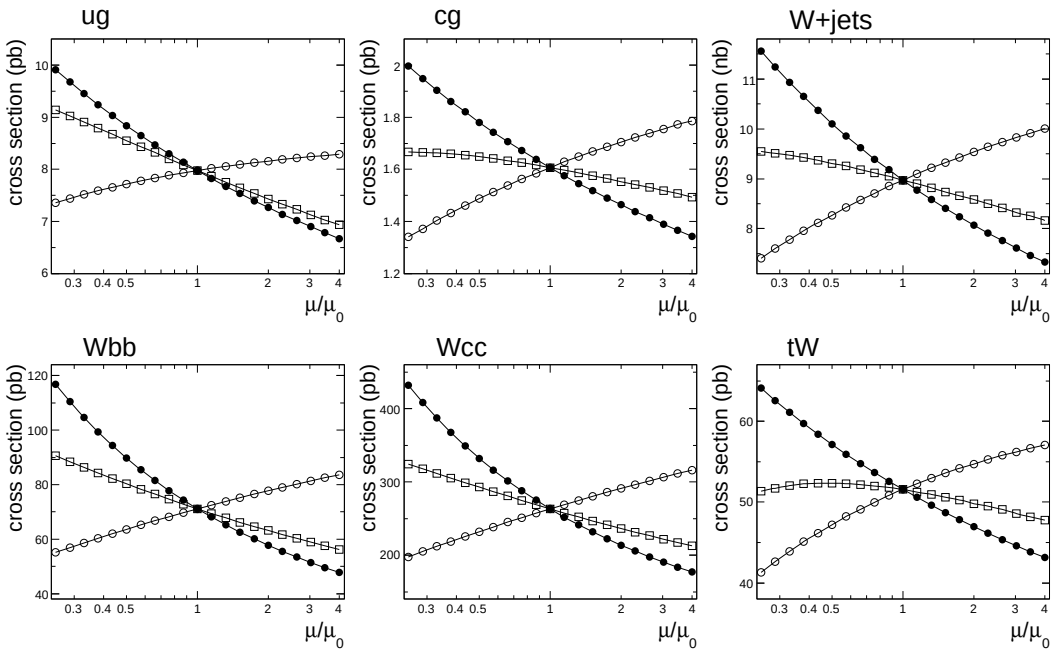

Figure 6: Dependence of the predicted cross section on scale variations for various processes: $\mu_{\rm R}$ only (closed circles), $\mu_{\rm F}$ only (open circles), and $\mu_{\rm R}$=$\mu_{\rm F}$ (squares). The statistical error at each point is typically $\sim 0.1\%$.

Table 4: Theoretical systematic uncertainty on leading-order cross sections.

process	$\delta\mu_{\rm R}$	$\delta\mu_{\rm F}$	PDF	$\delta m_t(\pm 2$ GeV/$c^2)$	Total
ug	$^{+10.8}_{-\ 8.9}\%$	$^{+\ 2.3}_{-\ 3.2}\%$	$\pm 12.0\%$	$^{+1.64}_{-1.56}\%$	$^{+16.4}_{-15.4}\%$
cg	$^{+10.8}_{-\ 8.9}\%$	$^{+\ 6.1}_{-\ 7.4}\%$	$\pm 11.3\%$	$^{+2.15}_{-2.02}\%$	$^{+16.9}_{-16.3}\%$
W+jets	$^{+12.6}_{-10.1}\%$	$^{+\ 6.1}_{-\ 7.4}\%$	$\pm\ 8.6\%$	-	$^{+16.5}_{-15.4}\%$
$Wb\overline{b}$	$^{+26.2}_{-18.8}\%$	$^{+\ 9.3}_{-10.5}\%$	$\pm\ 6.0\%$	-	$^{+28.4}_{-22.4}\%$
$Wc\overline{c}$	$^{+26.2}_{-18.8}\%$	$^{+10.7}_{-11.8}\%$	$\pm\ 5.3\%$	-	$^{+28.8}_{-22.8}\%$
tW	$^{+10.8}_{-\ 8.9}\%$	$^{+\ 6.0}_{-\ 8.4}\%$	$\pm 26.3\%$	$^{+3.04}_{-3.03}\%$	$^{+29.2}_{-29.2}\%$

5.2 Modelling of ISR and FSR

Emission of initial state radiation (ISR) and final state radiation (FSR) can have considerable effects on the overall kinematics. The effect in the case of signal processes is particularly dramatic. To estimate the effect of these parton showers, two independent data samples were simulated with ISR or FSR switched off.

Since the knowledge of these showers is of the order 10%, we conservatively take the 20% [20] of the efficiency difference to estimate the systematic uncertainty, i.e. 21% (signal) and 9% (background) for ISR-off, and 9% (signal) and 3% (background) for FSR-off. The systematic uncertainties on the coupling is then taken symmetrically to be *half* of the deviations, namely $\pm$ 3.5% (ISR) and $\pm$ 1.8% (FSR).

5.3 b-tagging performance

The results in this paper were obtained assuming a nominal b-tagging performance scenario with 60% b-tagging efficiency and charm and light-jet rejection factors independent of the jet transverse momentum. To estimate the systematic uncertainty due to b-tagging performance, we have in addition investigated the effect of using p_{T}-dependent rejection factors, as well as different b-tagging efficiencies (see Table 5).

Table 5: ATLFAST b-tagging performance scenarios used for systematic studies. The b-tagging efficiency and the charm and light-jet rejection factors are shown. It is also indicated whether the rejection is p_{T}-dependent or not. In the case of p_{T}-dependent rejections, the average rejections are shown. The first scenario shown is the nominal performance assumed throughout this paper.

$\varepsilon_{\text{b-tag}}$	R_c	R_{udsg}	Is R p_{T}-dependent?
60%	10	100	No
60%	6.7	93	Yes
50%	10.9	231	Yes
70%	4.3	34.1	Yes

The results obtained with the p_{T}-dependent rejection factors and 60% efficiency are not significantly different from the nominal results, therefore establishing that the approximation of p_{T}-independent rejection factors is realistic. (We note in addition, that recent ATLAS studies indicate that improved b-tagging methods can achieve a light-jet rejection factor of 150 ± 20 for the same 60% efficiency [21]. There is thus a good prospect of further increasing the sensitivity to the signal.)

Two other scenarios, with 50% and 70% efficiency were also compared to the nominal scenario. If the $\varepsilon_{\text{b-tag}} = 50\%$ scenario (jet rejections as in Table 5) is used, the relative drop in the total efficiencies for signal and background are 16% and 35%, respectively. In contrast, when the $\varepsilon_{\text{b-tag}} = 70\%$ scenario is used, the efficiencies increase by 14% and 65%, respectively. The systematic uncertainty due to b-tagging performance is taken directly from the deviations observed when using the 50% and 70% efficiency scenarios, and is calculated to be $^{+5.9}_{-2.4}\%$.

5.4 Jet energy scale

The absolute scale needed for jet energy calibration (both b-jets and light-jets, i.e. u, d, s, g) in ATLAS could be determined to an accuracy of 1% [2]. Here we assume a 3% uncertainty on b-jet energy scale, and for light-jets, 1%. Data samples were generated by rescaling the jet energy globally, and separately for b-jets and light-jets. The effect of such miscalibrations is very small: $< 0.5\%$ on the sensitivity on the coupling. For the sake of comparison, if we assume a 10% uncertainty on the energy scales, then the induced uncertainty would be about 3% (b-jet) and 0.3% (light-jet). Note that this is still smaller than the uncertainty due to the prediction of the signal cross section.

5.5 Pile up

At the LHC, there will often be more than one proton-proton interaction when the proton beams cross, owing to the high luminosity—these multiple pp interactions are said to be 'piling up'. At low luminosity ($\mathcal{L} = 10^{33}$ cm^{-2}s^{-1}), there will be an average of 2.3 pile up

events coming from non-diffractive inelastic interactions for every bunch crossing ($\sigma_{\text{pile}} =$ 70 mb)[2].

To estimate the systematic effect, a number of pile up events, distributed according to the Poisson distribution with a mean of 2.5 events, were added to each simulated physics event. The slightly higher mean number is due to the larger cross section for pile up, which includes double and single diffractive interactions (79.3 mb) as calculated by the tuned PYTHIA 6.226. The sensitivity limit on the coupling is weakened by +3.5% when pile up events are added, which is taken to be the systematic uncertainty.

5.6 Luminosity

Uncertainty in the measurement of the luminosity will propagate to the sensitivity on κ as $\frac{\Delta\kappa}{\kappa} = \frac{1}{4}\frac{\Delta L}{L}$, where $L = \int \mathcal{L}\, dt$. Therefore, assuming an uncertainty in L of 5%, the induced systematic uncertainty is 1.25% on κ and 2.5% on BR($t \to qg$).

5.7 Summary of systematic uncertainties

A summary of all the systematics studied is given in Table 6, for Scenario 1. The total systematic uncertainty on the derived sensitivity to coupling κ is estimated to be $^{+12}_{-10}$%. It has been checked [3] that this systematic uncertainty is valid for Scenarios 2 and 3 as well.

Table 6: Summary of systematic uncertainties.

Source	Uncertainty $\Delta\kappa/\kappa$
$\Delta\sigma_s$	$^{+8.3}_{-7.8}$%
$\Delta\sigma_b$	$^{+3.4}_{-3.1}$%
ISR	± 3.5%
FSR	± 1.8%
b-tagging performance	$^{+5.9}_{-2.4}$%
b-jet energy (± 3%)	± 0.3%
light-jet energy (± 1%)	± 0.4%
pile up (2.5 events)	+ 3.5%
luminosity (± 5%)	± 1.25%
Total	$^{+12.03}_{-\ 9.67}$%

The systematic uncertainty on the corresponding branching ratio is double the amount (as BR($t \to qg$) $\propto (\kappa_g^q/\Lambda)^2$, to first approximation). The dominant uncertainty is coming from the theoretical uncertainty on the signal cross section, which can be traced to the strong dependency of the cross section on the choice of PDF and the renormalization scale. The final results including the systematic uncertainty are presented in Table 9.

6 Conclusion

Many models beyond the standard model predict a strong enhancement of the top quark FCNC coupling. In particular, the tqg coupling ($q = u, c$), if large, can induce flavour-changing top quark production, $u(c) + g \to t$, which could be observed by ATLAS. This

Table 7: ATLAS's sensitivity to FCNC single top production for 10fb^{-1}, including systematic uncertainties.

		5σ	95% CL
Scenario 1	κ_g^q/Λ (TeV^{-1})	$\geqslant 0.0120^{+0.0014}_{-0.0012}$	$< 0.0069^{+0.0008}_{-0.0007}$
Scenario 2	κ_g^u/Λ (TeV^{-1})	$\geqslant 0.0138^{+0.0017}_{-0.0013}$	$< 0.0079^{+0.0010}_{-0.0008}$
Scenario 3	κ_g^c/Λ (TeV^{-1})	$\geqslant 0.0238^{+0.0030}_{-0.0023}$	$< 0.0137^{+0.0017}_{-0.0013}$
Scenario 1	BR$(t \to ug)$ + BR$(t \to cg)$	$\geqslant (2.64^{+0.63}_{-0.51})\times 10^{-4}$	$< (8.67^{+2.09}_{-1.68})\times 10^{-5}$
Scenario 2	BR$(t \to ug)$	$\geqslant (1.76^{+0.42}_{-0.34})\times 10^{-4}$	$< (5.80^{+1.37}_{-1.12})\times 10^{-5}$
Scenario 3	BR$(t \to cg)$	$\geqslant (5.21^{+1.32}_{-1.03})\times 10^{-4}$	$< (1.72^{+0.43}_{-0.34})\times 10^{-4}$

study shows that ATLAS is capable of observing such anomalous single top production with 5σ significance given 10 fb^{-1} of data (one year of low luminosity run), if $\kappa_g^q/\Lambda \geqslant 0.012$ TeV^{-1}, or BR$(t \to ug)$ + BR$(t \to cg) \geqslant 2.64\times 10^{-4}$. In terms of cross section, this requires a minimum of 13.7 pb of single top production via anomalous FCNC couplings. If no signal is found, ATLAS will be able to improve the current anomalous coupling (branching ratio) limits [22] by about a factor of 5–11 (22–116). The systematic uncertainty on κ_g^q/Λ is conservatively estimated to be $^{+12}_{-10}$%, and is twice as much for the corresponding branching ratio.

Acknowledgement

We thank members of the ATLAS Collaboration for useful discussions. This work is done using tools which are a result of collaboration-wide efforts. We would also like to thank S.R. Slabospitsky, co-author of the TOPREX generator, and Rui Santos for technical help and useful physics discussions. TLC acknowledges support from an ORS Award, a College Research Studentship, RHUL, and the Department of Physics, RHUL.

References

[1] For recent reviews, see e.g. F. Larios, R. Martínez, and M.A. Pérez, Int. J. Mod. Phys. A 21 (2006) 3473 [hep-ph/0605003]; J.A. Aguilar-Saavedra, Acta Phys. Polon. B 35 (2004) 2695 [hep-ph/0409342].

[2] ATLAS Collaboration, *ATLAS Detector and Physics Performance*, Technical Design Report, CERN/LHCC/99-14 (1999).

[3] T.L. Cheng, *Search for Anomalous Single Top Quark Production via Flavour-Changing Neutral Currents with the ATLAS Detector at the Large Hadron Collider*, Ph.D. thesis, University of London (2007).

[4] O. Çakir and S.A. Çetin, J. Phys. G: Nucl. Part. Phys. 31 (2005) N1-N8.

[5] S.R. Slabospitsky and L. Sonnenschein, Comput. Phys. Commun. 148 (2002) 87 [hep-ph/0201292]; S.R. Slabospitsky, private communications, Sept. 2006.

[6] M. Beneke et al., 'Top quark physics', in *Proceedings of the workshop on standard model physics (and more) at the LHC*, CERN Report, 2000-004 (2000) pp. 419–529 [hep-ph/0003033].

[7] V.M. Abazov et al. (D0 Collaboration), Phys. Rev. Lett. 99 (2007) 191802 [arXiv:0801.2556].

[8] Z. Sullivan, Phys. Rev. D 70 (2004) 114012 [hep-ph/0408049].

[9] F. Derue and C. Sefron, *Electron/jet separation with DC1 data*, ATLAS Note, ATL-PHYS-PUB-2005-016 (2005).

[10] T. Sjöstrand et al., Comput. Phys. Commun. 135 (2001) 238 [hep-ph/0010017];
T. Sjöstrand, L. Lönnblad, and S. Mrenna, *PYTHIA 6.2 Physics and Manual* [hep-ph/0108264].

[11] H.L. Lai et al., Eur. Phys. J. C 12 (2002) 375 [hep-ph/9903282].

[12] A. Moraes, C. Buttar, and I. Dawson, *Prediction for minimum bias and underlying event at LHC energies*, ATLAS Note, ATL-PHYS-PUB-2005-007 (2005).

[13] E. Richter-Was, D. Froidevaux, and L. Poggioli, *ATLFAST 2.0 a fast simulation package for ATLAS*, ATLAS Note, ATL-PHYS-98-131 (1998).

[14] S. Eidelman et al., Phys. Lett. B 592 (2004) 1.

[15] See e.g. M.H. Seymour, *Quantum Chromodynamics* [hep-ph/0505192].

[16] A.D. Martin, R.G. Roberts, W.J. Stirling, and R.S. Thorne, Phys. Lett. B 531 (2002) 216 [hep-ph/0201127].

[17] A.D. Martin, R.G. Roberts, W.J. Stirling, and R.S Thorne, Eur. Phys. J. C 28 (2003) 455 [hep-ph/0211080].

[18] The Tevatron Electroweak Working Group, *Combination of CDF and DØ results on the mass of the top quark* [arXiv:0803.1683].

[19] P. Nason et al., 'Bottom production', in *Proceedings of the workshop on standard model physics (and more) at the LHC*, CERN Report, 2000-004 (2000) pp. 232–238 [hep-ph/0003142].

[20] See e.g. F. Hubaut et al., Eur. Phys. J. C 44 s02 (2005) 13.

[21] S. Corréard, V. Kostioukhine, J. Levêque, A. Rozanov, and J.B. de Vivie, *b-tagging with DC1 data*, ATLAS Note, ATL-PHYS-2004-006 (2004).

[22] Current limits on couplings are from Ref. [7], while the limits on the branching fractions are inferred using the TOPREX generator.